Adsorptive removal of methyl orange and methylene blue from aqueous solutions with *Acacia crassicarpa* activated carbon

Tue Ngoc Nguyen[1*], Khanh Quoc Dang[2], Duc Trung Nguyen[1]

[1]School of Chemical Engineering, Hanoi University of Science and Technology
[2]School of Materials Science and Engineering, Hanoi University of Science and Technology

Abstract:

In this study, activated carbon prepared from *Acacia crassicarpa* bark was prepared and studied for the potential development of low-cost, carbon-based adsorbents that remove industrial dyes from aqueous solutions. Various spectroscopy techniques and surface analyses were used to characterize the adsorbents. The adsorption of methyl orange (MO) and methylene blue (MB) onto the material was investigated under optimal experimental conditions including temperature, adsorbent dosage, and initial concentration of chemicals. The Langmuir isotherm model was observed to fit the adsorption data well. The maximum adsorption capacities predicted by the Langmuir isotherm were found to be 10.36 mg.g^{-1} for MO and 15.34 mg.g^{-1} for MB. The adsorbents were better able to remove the cationic dye than the anionic dye. The results of this study will be useful for future scale-up production of low-cost adsorbents using *Acacia crassicarpa* for the removal of cationic and anionic dyes.

Keywords: adsorption, carbon, dyes, equilibrium, porous materials.

Classification number: 2.2

Introduction

A germ-free environment and safe drinking water are fundamental necessities that support healthy life. Currently, clean water is a vital element of domestic usage and it is employed in industrial and agricultural applications. However, existing suitable water sources can be contaminated by bacteria, microbes, and/or industrial waste containing organic pollutants, heavy metals, and various anions [1-5]. Two of the most commonly used dyes in biology, medicine, and textile industries are the chemical indicators MB and MO, both of which can cause various health problems like abdominal disorders if digested [6, 7]. Additionally, the presence of MB and MO in water, even at low concentrations, can absorb a major portion of sunlight and thus reduce sunlight penetration that can decrease the dissolved oxygen in water and hinder the growth of aquatic biota [6, 8]. Therefore, it is crucial to remove MB and MO dye molecules from industrial effluent before being discharged into the environment. Therefore, removing dyes from aqueous solutions has become an immense challenge that has attracted great interest.

Various physical, chemical, and even biological techniques such as biosorption, chemical oxidation, coagulation, membrane filtration, photodegradation, and adsorption have been employed to remove these organic pollutants from aqueous environments. However, adsorption has been known as the most effective, simple, and inexpensive technique as it is one of the most studied dye removal methods for water treatment [9, 10]. Recently, carbon-based materials like activated carbon (AC) have been used extensively as adsorbents due to their advantages in specific surface area, weight, mechanical strength, and electronic characteristics. With the purpose of improving the performance of carbon-based materials, a number of studies employing AC originating from low cost agricultural waste have been established [11]. Among biomass and agricultural wastes, *Acacia crassicarpa* bark is one alternative low cost material that can be used for AC preparation. Not only does this precursor have a large organic content and is locally available, there are large amounts of this agricultural waste available from industries that can be transformed into a value-added product. In addition, only small sample sizes of coffee grounds are needed to prepare the activation process. To the best of our knowledge, no studies of *Acacia crassicarpa* activated carbon (ACAC) have been published for MB and MO adsorption.

[*]Corresponding author: Email: tue.nguyenngoc@hust.edu.vn

Based on these factors, this paper aims to prepare and evaluate the dye removal potential of a novel, low cost, and green activated carbon originating from *Acacia crassicarpa* bark for removing MO and MB dyes from aqueous solutions. Two dye wastewaters containing MO and MB were adsorbed by the materials and the equilibrium of the dye adsorption process was thoroughly studied. The obtained results were used to assess the adsorption isotherm of the materials to determine optimal parameters.

Materials and method

Experimental materials

The chemicals used herein were all commercial products. All chemical reagents were of analytical grade and used without further purification. Chemicals were purchased from the Xilong Company in China. MB and MO, which have the chemical formula of $C_{16}H_{18}ClN_3S$ (MW of 319.85 g.mol^{-1}, λ_{max} of 668 nm) and $C_{14}H_{14}N_3NaO_3S$ (MW of 327.33 g.mol^{-1}, λ_{max} of 464 nm), respectively, were selected as the adsorbates in this research work.

Preparation of AC

Preparation of AC from *Acacia crassicarpa* bark: *Acacia crassicarpa* bark was collected from Nghe An Province, Viet Nam. The collected bark were washed several times with distilled water to remove any dirt. It was then air dried at 105°C for 24 h to a constant weight. The obtained dried solids were ground into a fine powder and then sieved to 43 µm. Then, the dried powder was loaded into a programmable tube furnace and heated up to 400°C under purified Ar gas flow (120 cm^3.min^{-1}) for organic phase removal. The resulting solid was denoted as ACAC-1. The next step was the carbonization process. First, the precursor was introduced to a sample holder that was placed in a rotary tube furnace. The operating conditions were increased from room temperature to 600°C with a pre-selected heating rate of 2, 3, and 4°C min^{-1} under Ar flow of 30 ml.min^{-1}. At 600°C, the temperature was subsequently increased to 1150°C with a heating rate of 5°C min^{-1} and was kept fixed for 1 h. The corresponding AC from the three different temperature rates were denoted as ACAC-2, ACAC-3, and ACAC-4 for 2, 3, and 4°C min^{-1}, respectively. The four samples then were measured using X-ray diffraction (XRD), Brunauer-Emmett-Teller (BET) analysis, and elemental analysis. After that, the ACAC-3 sample underwent a second carbonization process in which the temperature was first increased to 600°C and then increased to 1160°C with heating rates of 3°C min^{-1} and 5°C min^{-1}, respectively. The resulting solid was denoted as ACAC-5. Sample ACAC-5 was then carbonized with the same procedure as the previous ACAC-3. The resulting AC sample was denoted as ACAC-6. Afterward, all AC samples were washed with distilled water repetitively for 24 h until the sample colour was unchanged. The washed carbon was impregnated with NaOH 10% with a ratio of 1:5, then washed again with distilled water until pH 7 and vacuum-dried at ambient temperature (20°C) to become activated carbon.

Characterization of the AC

Elemental analysis integrated with IR spectroscopy was used to determine the components of the synthesized ACs. BET measurements were conducted to measure the surface area of all the AC samples. Scanning electron microscopy (SEM) was used to observe the surface morphology and surface texture of the materials. To study the changes in the microstructures of the four AC samples, an analysis was performed on measurements from high-resolution XRD. The carbon content was determined from IR measurements on a CS744 carbon/sulfur analyser via combustion.

Adsorption experiments

First, we chose two different dyes, MB and MO, to test the adsorption performance of the selected adsorbents. MB showed a positive charge in solution as it is a cationic dye, while MO showed a negative charge in solution as it is an anionic dye. A temperature of 25°C and pH of 7.0 were fixed throughout all experiments. First, 2.0-3.0 mg of the adsorbents were dispersed into 50 ml each of two dyes with various initial concentrations. Volumetric flasks were ultrasonicated for 1 h, then shaken in a gas bath thermostatic oscillator with a shaking speed of 300 rpm until equilibrium was reached. When the adsorption equilibrium was reached, the amount of residual dye concentration was determined at their specific wavelength (664 nm for MB and 464 nm for MO) using a UV-Vis spectrophotometer. The concentrations of the dyes were estimated using linear regression equations obtained by plotting its calibration curve. The amount of the two dyes adsorbed by the adsorbent (q_e, mg.g^{-1}) was calculated by the following mass balance formula:

$$q_e = \frac{(C_o - C_e)V}{W}$$

where C_0 (mg.l^{-1}) and C_e (mg.l^{-1}) are the initial and equilibrium concentrations of MB or MO, respectively, V is the volume of the solution (L), and M is the weight of the adsorbent (g). The two isotherm models of Freundlich and Langmuir were used to evaluate the adsorption equilibrium characteristics of MB and MO on the two carbon-based materials. All isotherm models were fit to experimental data using linear equations, which are shown in Table 1.

Table 1. Adsorption isotherm models and their linear equations

Isotherm models	Equations
Langmuir adsorption isotherm	$\frac{C_e}{q_e} = \frac{1}{q_{max}k_L} + \frac{C_e}{q_{max}}$
Freundlich adsorption isotherm	$\log q_e = \log K_F + \frac{1}{n}\log C_e$

In the equations of Table 1, q_{max} (mg.g^{-1}) is adsorption constant related to the adsorption capacity, k_L (l.g^{-1}) is the adsorption constant related to the energy of adsorption, K_F is the adsorption constant related to adsorption capacity (mg.g^{-1}) (l.mg^{-1})$^{1/n}$ and n is the adsorption constant measuring the adsorption intensity.

Results and discussion

As mentioned above, the structural characteristics of the ACAC samples were analysed using SEM, BET, and the CS744 carbon/sulfur analyser.
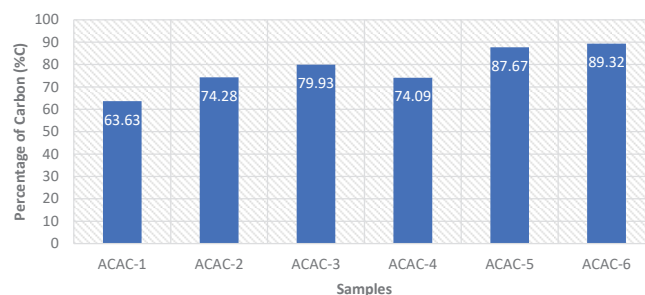
Elemental analysis

The carbon contents of the ACAC samples are presented in Fig. 1. According to the IR measurement of the CS744 carbon/sulfur analyser, the different heating rates of ACAC-1 to ACAC-4 lead to different carbon contents that increased from 63.63 to 79.93%, respectively. Sample ACAC-3 was then selected to proceed further because of its high carbon content. After two carbonization processes on ACAC-4, 89.32% C was achieved.

Pre-treatments were applied prior to the carbonization process to ensure the stability and preservation of the precursor structure during the subsequent carbonization. In fact, specialized pre-treatments can be used to enhance the carbon content in prepared materials in terms of stability and separation performance. The first carbonization process facilitates stabilization of the precursor's asymmetric structure and provides dimensional stability in order to withstand the high temperatures of the subsequent carbonization steps. In the following carbonization process, mostly heteroatoms existing in polymeric macromolecules were removed and subsequently a stiff and cross-linked carbon matrix was obtained. The carbon matrix with an amorphous porous structure formed from the evolvement of gaseous products and the reconfiguration of the crystalline structure during carbonization.

On the other hand, the variation of carbon content in the ACAC samples represents an interaction between temperature and heating rate on the yield of carbon content. The carbonization of the AC at 600°C is dominated by the depolymerization reaction and decomposition of volatile matter to form solid carbon. The heating rate affects the rate of volatile evolution from the bark. In more detail, heating rates at temperatures above 400°C favour rapid volatile evolution. The resulting carbon content comes from the process that dominates, i.e., either the formation of solid carbon or the removal. A lower heating rate therefore allows equilibrium reactions to promote higher carbon content. With an increase in heating rate up to 3°C.min^{-1}, the condensation reaction dominates the carbonization process and the fixed carbon content continues to rise. As seen in Fig. 1, the carbon content tends to increase when the temperature was below 600°C and the heating rate was less than 3°C.min^{-1}. When the heating rate rose above 3°C.min^{-1}, the carbon content decreased from 79.93% for ACAC-3 to 74.09% for ACAC-4. The reason being is that at high heating rates, molecular disruption is steadfast and volatile fragments are consequently released so quickly that successive adjustments and equilibrium, leading to further primary reactions that yield char, have less opportunities to take place. When the heating rate rises further, the condensation reaction gradually slows down and the rate of formation of fixed carbon decreases, these processes are accompanied with the result of reduced fixed carbon content.

Fig. 1. The percentage of carbon element in the six ACAC samples.

To study changes in the microstructures of the ACAC samples, XRD analysis was carried out. As shown in Fig. 2, the ACAC samples all primarily contained carbon and calcium carbonate (18.18, 34.15, 47.17, and 50.96° according to the JCPDS:01-078-4614). From the XRD spectrum, ACAC-1 does not exhibit distinct peaks corresponding to a typical carbon material, thus, no discrete mineral phase was formed. Additionally, the hump in the 2θ range from 20 to 30° suggests a high degree of disorder in the carbonaceous material. Thus, ACAC-1 has a completely amorphous structure as expected with organic materials. In the XRD spectra of ACAC-3 and ACAC-4, a distinct peak of carbon appears that corresponds to the presence of crystal phase. After the carbonization processes, ACAC-5 and ACAC-6 show very well defined peaks of carbon at 2θ values of 26.26, 29.20, 43.27, 47.26, and 48.52° (reference to the patterns JCPDS:04-019-9068, 01-089-8495, 04-007-2136, and 04-013-5952). These diffraction peaks indicate that these samples have a turbostratic structure.
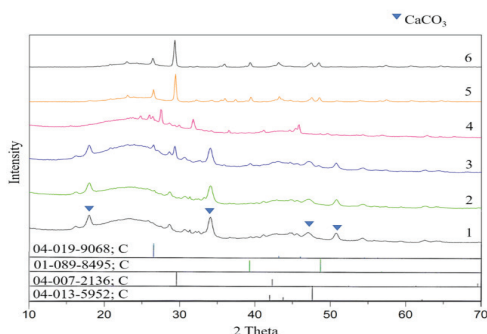
Fig. 2. XRD spectra of ACAC with four different settings. Numbers 1 through 6 represent the six ACAC samples.
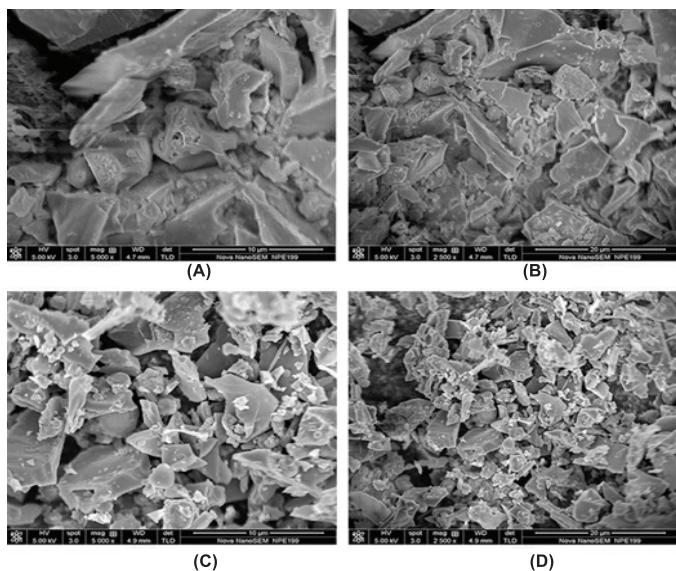

Fig. 3. SEM micrographs of four the ACAC samples: (A) and (B) are ACAC-1; (C) and (D) are ACAC-4.

Figure 3 is an SEM image of the ACAC samples before and after the first carbonization process, respectively. A porous structure of the ACAC samples was not clearly observed by SEM and their surface is also covered by significant amount of impurities. Using ImageJ software, the particle size fraction of ACAC-1 from Fig. 3 was 3.51 µm and the particle size fraction of ACAC-4 was 1.84 µm. This suggests that the surface area of ACAC-4 increased in comparison to ACAC-1. Based on these results, ACAC-4 went through two carbonization processes and the surface area of the final product was measured by the BET method.

The pore structure analysis

The pore size distributions of ACAC-6 were analysed and the summarized results are presented in Fig. 4. The diameter of a copper atom is roughly 0.257 nm, and since the average pore diameter of ACAC is 10 µm, the copper atoms easily remain in the pores of the activated carbon. Sample ACAC-6 showed an average S_{BET} of 363.56 m^2.g^{-1}. According to the obtained results, the adsorption capacity of the adsorbent was determined to not only depend on surface properties, but also pore structure. The use of ultrasonic power can contribute to making new pores on

the surface of activated carbon, which improves MB removal. Besides, as shown in Fig. 4, most of the pores fall into a diameter category of 1-2.5 µm. According to Kasaoka, et al., the pore diameter of an adsorbent must be at least 1.7 times larger than the adsorbate so that adsorption becomes possible [12]. In this case, the diameters of both MB and MO are about 0.8 nm, while the average pore size of ACAC is 2.00 µm; thus, it can efficiently adsorb both MB and MO molecules.
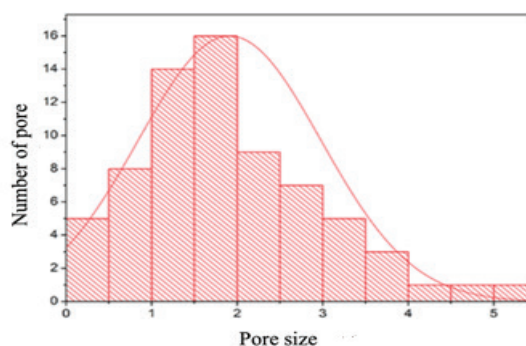

Fig. 4. The distribution of the pores and their sizes in sample ACAC-6.

Adsorption isotherm

As mentioned before, the adsorption isotherm is a vital tool that explains the relationship between adsorbate molecules and the adsorbent surface. It describes how adsorbate molecules are distributed on the surface of the adsorbent. The obtained parameters from the two models for ACAC-6 are summarized in Table 2. From the results, the correlation coefficient (R^2) of the Langmuir isotherm is the largest, which indicates that adsorption depends on the interaction between the homogeneous and the monolayer coverage of MB and MO onto the two studied materials. Additionally, a characteristic parameter of the Langmuir isotherm was also determined, i.e., the dimensionless factor R_L also known as the separation factor, which can be calculated by the following equation:

$$R_L = \frac{1}{1 + K_L C_0}$$

where C_0 is the initial concentration of MB (or MO) and k_L is the Langmuir constant.

Table 2. Langmuir and Freundlich parameters for MB and MO adsorption on the ACAC-6.

	Langmuir coefficients		
Adsorbates	q_m (mg.g^{-1})	K_L (l.g^{-1})	R^2
MB	15.34	1.11	0.9921
MO	10.36	1.04	0.9104
	Freundlich coefficients		
	n	K_F	
MB	3.66	8.14	0.8922
MO	2.96	3.87	0.6070

The value of R_L is associated with the type of isotherm: unfavourable ($R_L>1$), linear ($R_L=1$), favourable ($0<R_L<1$), or irreversible ($R_L=0$) [13]. The R_L values of MB adsorption onto activated carbons are determined to be in the range of 0.04-0.15 for ACAC-6, which represents that the Langmuir adsorption isotherm is favourable. The Langmuir and Freundlich isotherms for MB and MO adsorption onto ACAC-6 are shown in Fig. 5 and Fig. 6, respectively.
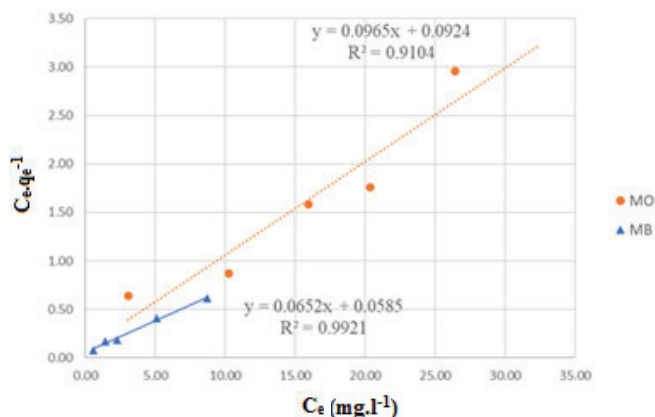

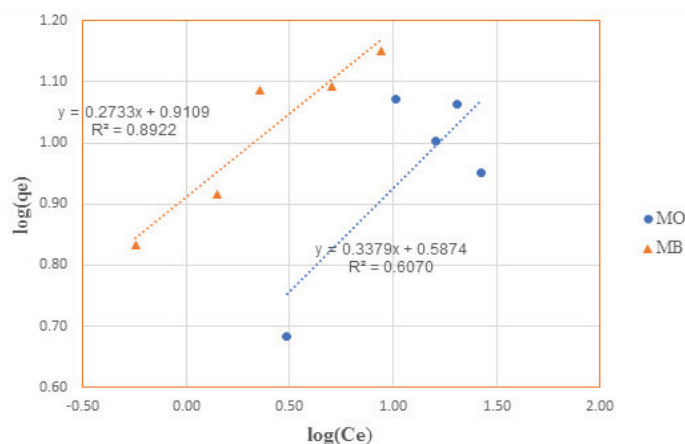**Fig. 5. Langmuir adsorption isotherm for MB and MO removal using ACAC-6.**

Fig. 6. Freundlich adsorption isotherm for MB removal using ACAC-6.

Conclusions

The removal of the industrial dyes MB and MO by using activated carbon originating from *Acacia crassicarpa* agricultural waste was investigated. Adsorption experiments were performed and the maximum adsorption capacity was determined by the adsorption of MB and MO. The experimental data fit the Langmuir isotherm model indicating a monolayer distribution of dye molecules over the surface of the activated carbon. The Langmuir maximum adsorption capacity was determined as 15.34 mg.g^{-1} for MB and 10.36 mg.g^{-1} for MO. Based on all results, ACAC can be regarded as a potential adsorbent for the removal of MB dye from aqueous solutions.

COMPETING INTERESTS

The authors declare that there is no conflict of interest regarding the publication of this article.

REFERENCES

[1] I. Ismail, et al. (2012), "Combined coagulation flocculation pre treatment unit for municipal wastewater", *J. Adv. Res.*, **3(4)**, pp.331-336.

[2] M. Ghaedi, et al. (2015), "Characterization of zinc oxide nanorods loaded on activated carbon as cheap and efficient adsorbent for removal of methylene blue", *J. Ind. Eng. Chem.*, **21**, pp.986-993.

[3] M. Ibrahim, et al. (2009), "Removal of COOH, Cd and Pb using water hyacinth: FTIR and flame atomic absorption study", *J. Iran. Chem. Soc.*, **6(2)**, pp.364-372.

[4] G. Sharma, et al. (2018), "Fabrication and characterization of Gum arabic-cl-poly(acrylamide) nanohydrogel for effective adsorption of crystal violet dye", *Carbohydr. Polym.*, **202**, pp.444-453.

[5] M. Naushad (2014), "Surfactant assisted nano-composite cation exchanger: development, characterization and applications for the removal of toxic Pb^{2+} from aqueous medium", *Chem. Eng. J.*, **235**, pp.100-108.

[6] M. Zubair Alam, et al. (2010), "Mutagenicity and genotoxicity of tannery effluents used for irrigation at Kanpur, India", *Ecotoxicol. Environ. Saf.*, **73(7)**, pp.1620-1628.

[7] M. Bahrami, et al. (2015), "Effect of the supported ZnO on clinoptilolite nano-particles in the photodecolorization of semi-real sample bromothymol blue aqueous solution", *Mater. Sci. Semicond. Process.*, **30**, pp.275-284.

[8] S. Sohrabnezhad, et al. (2010), "Comparison absorption of new methylene blue dye in zeolite and nanocrystal zeolite", *Desalination*, **256(1)**, pp.84-89.

[9] C. Leodopoulos, et al. (2012), "Single and simultaneous adsorption of methyl orange and humic acid onto bentonite", *Appl. Clay Sci.*, **70**, pp.84-90.

[10] M. Rafatullah, et al. (2009), "Adsorption of copper (II), chromium (III), nickel (II) and lead (II) ions from aqueous solutions by meranti sawdust", *J. Hazard. Mater.*, **170(2)**, pp.969-977.

[11] K. Bedin, et al. (2016), "KOH-activated carbon prepared from sucrose spherical carbon: adsorption equilibrium, kinetic and thermodynamic studies for Methylene Blue removal", *Chem. Eng. J.*, **286**, pp.476-484.

[12] S. Kasaoka (1987), "Design of molecular sieving carbon-studies on adsorption of various dyes in liquid phase", *Nippon Kagaku Kaishi*, **1**, pp.2260-2266.

[13] S. Guo, et al. (2009), "Kinetics and equilibrium adsorption study of lead(II) onto the low cost adsorbent-Eupatorium adenophorum spreng", *Process Saf. Environ. Prot.*, **87(5)**, pp.343-351.